

Self-trapping of negative ions due to electron detachment in the afterglow of electronegative gas plasmas

I. D. Kaganovich, B. N. Ramamurthi, and Demetre J. Economou^{a)}

Plasma Processing Laboratory, Department of Chemical Engineering, University of Houston, Houston, Texas 77204-4792

(Received 29 December 1999; accepted for publication 20 March 2000)

The spatiotemporal evolution of charged species densities and wall fluxes during the afterglow of an electronegative discharge has been investigated. It was found that plasma decay crucially depends on the product of negative-ion-detachment frequency (γ_d) and diffusion time τ_d . If $\gamma_d\tau_d > 2$, negative ions convert to electrons during their diffusion towards the walls. The presence of detached electrons results in “self-trapping” of the negative ions, due to emerging electric fields, and the negative-ion flux to the walls is extremely small. Thus, negative ions can be extracted in the afterglow only if $\gamma_d\tau_d < 2$. © 2000 American Institute of Physics. [S0003-6951(00)00320-X]

Negative-ion-rich (electronegative) plasmas are of great importance in semiconductor manufacturing,¹ negative-ion sources,^{2,3} the *D* layer of the lower ionosphere,⁴ etc. There often appear new and interesting phenomena in plasmas containing negative ions in addition to electrons and positive ions; see, for example, Refs. 5–7.

Pulsed plasmas in electronegative gases have been shown to offer important advantages compared to their continuous-wave (cw) counterparts.^{1–3} Negative ions are difficult to extract from cw plasmas because of the electrostatic fields due to the presence of electrons. When power is turned off in the afterglow, however, electrons disappear because of diffusion to the walls and attachment to gas molecules. After some time in the afterglow, the electron density and temperature are too low for any significant electrostatic fields to exist, and a transition occurs from an electron-dominated plasma to a positive-ion–negative-ion (ion–ion) plasma.^{8–10} After that time, it is possible to extract negative ions out of the plasma. Nevertheless, there are situations for which the electron density in the afterglow does not decay to a level for the fields to completely disintegrate. An example is detachment of negative ions in the afterglow that generates new electrons. Under such circumstances it is possible for negative ions to remain trapped in the plasma. Conditions for this scenario to occur are studied in this letter by numerical simulation and mathematical modeling.

We assume that the ion mean-free path is smaller than the characteristic chamber dimension and examine one-dimensional species transport in a parallel-plate geometry. This study is applicable to plasmas that are not strongly electronegative (e.g., oxygen) and electron detachment can occur in the afterglow. The molecular-oxygen-ion mean-free path in an oxygen discharge at the lowest pressure studied (2 mTorr) is smaller than the interelectrode gap. The small mean-free path is due to the large cross section for resonant charge-exchange collisions. For a collisional plasma, the species fluxes are described by a drift-diffusion model, $\Gamma_k = -D_k \partial n_k / \partial x \pm \mu_k n_k e E$, where D_k and μ_k are the *k*-specie diffusion coefficient and mobility, respectively, tied by the

Einstein relation $D_k = T_k \mu_k$. T_k is the *k*-specie temperature. The self-consistent electrostatic field can be found from the condition of zero net current $j = e(\Gamma_p - \Gamma_n - \Gamma_e) = 0$, and is given by

$$E = \frac{D_p \nabla p - D_n \nabla n - D_e \nabla n_e}{\mu_p p + \mu_n n + \mu_e n_e}. \quad (1)$$

The symbols and subscripts *p*, *n*, and *e* correspond to positive ions, negative ions, and electrons, respectively. If the electron density ($\mu_e n_e \gg \mu_p p, \mu_n n$) and its gradient are not too small, electrons are described by Boltzmann equilibrium: $E = -(T_e/e) \nabla(\ln n_e)$. Equation (1) for the electric field along with the mass continuity equations for negative ions and electrons, the electroneutrality constraint, and an equation for the electron temperature yield a complete system of equations that describes the spatiotemporal evolution of charged-species densities, fluxes, and electric field.

$$\frac{\partial n}{\partial t} - \mu_n \frac{\partial}{\partial x} \left(T_i \frac{\partial n}{\partial x} + e E n \right) = \nu_{\text{att}} n_e - \gamma_d n - \beta_{ii} n p, \quad (2a)$$

$$\frac{\partial p}{\partial t} - \mu_p \frac{\partial}{\partial x} \left(T_i \frac{\partial p}{\partial x} - e E p \right) = Z_{\text{ioniz}} n_e - \beta_{ii} n p, \quad (2b)$$

$$n_e = p - n. \quad (2c)$$

In Eqs. (2a)–(2c), β_{ii} is the ion–ion recombination rate coefficient, and Z_{ioniz} , ν_{att} , and γ_d , are the ionization, attachment, and detachment frequencies, respectively. We impose the Bohm velocity for positive ions at the plasma-sheath boundary. The negative-ion flux is calculated as shown by Ashida and Lieberman.¹¹ Equations (2a)–(2c) are supplemented with an equation for the electron temperature.¹²

We have chosen a model electronegative gas based on oxygen chemistry.¹² We did not account for dissociation of oxygen molecules, assuming that the deposited power is small. The chemistry model was validated against experimental measurements of ion and electron density and their profiles in cw oxygen discharges.¹³

Figures 1 and 2 show typical results of negative-ion and electron densities, metastable singlet delta $a^1\Delta_g$ (O_2^*), and electron temperature at the discharge center, as well as the

^{a)}Electronic mail: economou@uh.edu

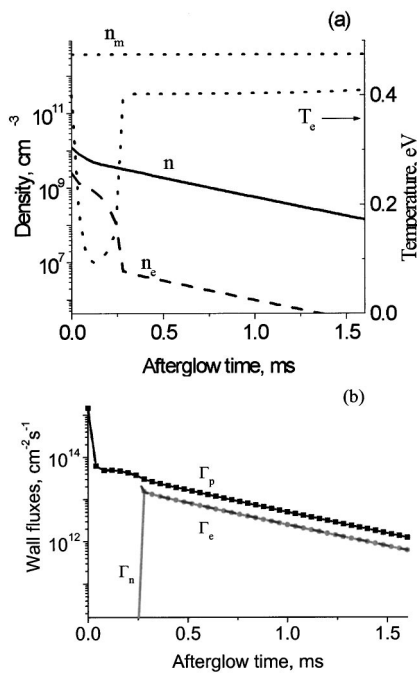


FIG. 1. Temporal evolution of plasma parameters in the afterglow of model electronegative gas based on oxygen: (a) densities at the center of the discharge; n : negative-ion density; n_e : electron density; n_m : metastable $a^1\Delta_g O_2^*$ density; T_e : electron temperature and (b) fluxes at the wall electron Γ_e , positive ion Γ_p , and negative ion Γ_n flux, respectively. Oxygen pressure $p=2$ mTorr, discharge interelectrode gap 10 cm, and average power density 10 mW/cm^3 .

charged species fluxes at the wall, all as a function of time in the afterglow (power is turned off at time 0). The only difference between Figs. 1 and 2 is the discharge pressure.

During the active glow (power on), negative ions are piled up in the interior of the vessel by the electric field in

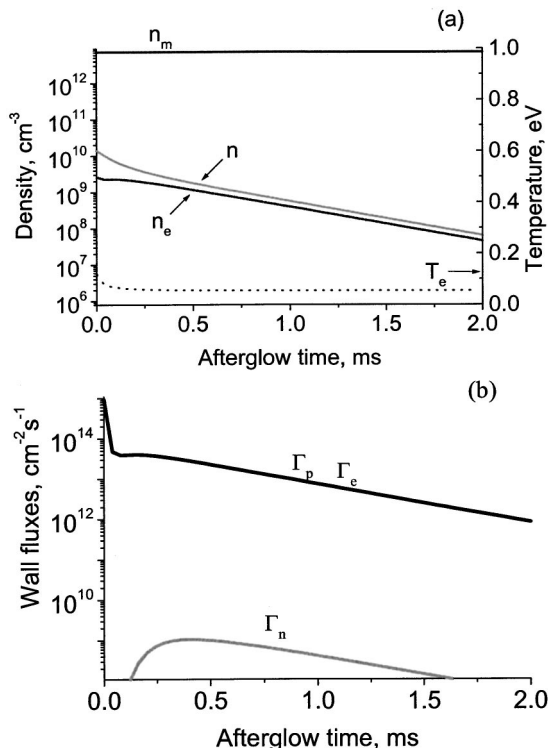


FIG. 2. All conditions are the same as in Fig. 1, except $p=4$ mTorr.

the plasma, and there is practically no negative-ion current to the wall. In the afterglow (power off), the electron temperature drops rapidly at first, mainly due to electron-impact excitation losses. Several tens of μs into the afterglow, the electron temperature has decreased from several eV (not shown) to practically room temperature. Thus, late in the afterglow high-threshold electron-impact reactions (excitation, ionization), as well as attachment, switch off. For the plasma parameters of Figs. 1 and 2, the main processes in the afterglow governing plasma dynamics are transport and detachment of negative ions due to collisions with metastable oxygen molecules¹⁴ O_2^* . Note that the concentration of metastables is large because of their low wall quenching probability ($\sim 10^{-3}$).

Comparing Figs. 1 and 2, one can see a drastic difference in behavior. In Fig. 1 (at 2 mTorr), the plasma is rapidly depleted of electrons. As a result, the plasma electronegativity (ratio of negative-ion density n to electron density n_e) increases and a transition occurs to a practically electron-free (ion-ion) plasma.^{8-11,14} This transition is abrupt [occurs just before 0.25 ms in Fig. 1(a)], accompanied by rapid escape of the remaining electrons by essentially free-electron diffusion. The electron density tends to nearly zero in a finite time, after which negative ions come out of the plasma and the negative-ion flux to the wall increases sharply [at 0.25 ms in Fig. 1(b)]. At a pressure of 4 mTorr, however, the temporal evolution of electron density and wall fluxes is completely different. The electron density does not decay as rapidly and the plasma electronegativity is not very large, to the point that the electric field is determined almost entirely by electrons (Boltzmann equilibrium). Negative ions are trapped in the vessel and the negative-ion flux is nearly zero during the entire afterglow [Fig. 2(b)].

In Fig. 1, the electron temperature rises slightly later in the afterglow since there is some energy deposited by the detached electrons (0.6 eV per event) and this energy is distributed to a very small number of electrons.

The metastable density does not change appreciably in the afterglow in Figs. 1 and 2, because there are no appreciable losses of metastables. For example, the rate of wall and electron quenching of metastables (dominant loss mechanisms) is of the order of 10–100 ms much smaller than the 2 ms time period shown. This also results in substantial metastable density in the discharge.

Theoretical analysis shows that the crucial parameter that controls behavior is $\gamma_d \tau_d$ —the product of negative-ion detachment frequency ($\gamma_d = K_d n_m$) and negative-ion free-diffusion time ($\tau_d = \Lambda^2 / D_n$). Here, $D_n = 6.9 \times 10^4 (\text{cm}^2 \text{ s}^{-1}) / P (\text{mTorr})$, $K_d = 3 \times 10^{-10} \text{ cm}^3 \text{ s}^{-1}$ is the rate constant for detachment,¹² n_m is the O_2^* density, and Λ is the effective ion-diffusion length.¹⁵ For a pressure $p=2$ mTorr, $\gamma_d \tau_d = 0.55$, while for $p=4$ mTorr, $\gamma_d \tau_d = 1.5$.

In Fig. 3, the maximum negative-ion flux during the afterglow is shown as a function of pressure. Beyond a pressure of 3.5 mTorr, the negative-ion flux is very small (by a few orders of magnitude). Thus, negative ions can be extracted in the afterglow only if the pressure is smaller than a critical value. The critical pressure depends on the values of other plasma parameters. It turns out that the critical pressure is determined by the condition $\gamma_d \tau_d \sim 1$.

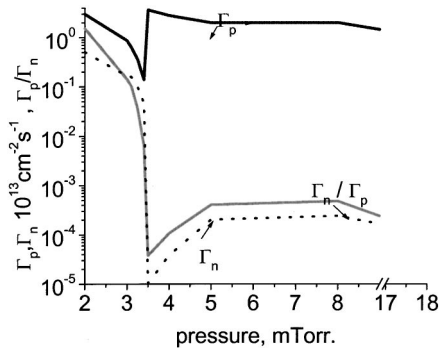


FIG. 3. Maximum of negative-ion flux in the afterglow as a function of pressure. All other conditions are the same as in Fig. 1.

Negative-ion self-trapping in the afterglow can be analyzed by a simplified model. We assume that the electron temperature in the afterglow is equal to the ion temperature $T_i = T_e \equiv T$, and that the ion mobilities are equal $\mu_n = \mu_p \equiv \mu_i$ for simplicity. We also assume that ion-ion recombination is slow compared to attachment/detachment and it can be neglected. Negative-ion detachment occurs via reactions with O_2^* .

For zero-density boundary condition for all charged species at the wall, the spatial profiles tend to the fundamental mode, after a short period in the afterglow: all three density profiles are similar:^{15,16}

$$\frac{\nabla n}{n} = \frac{\nabla p}{p} = \frac{\nabla n_e}{n_e} = \cos(\pi x/2L). \quad (3)$$

Substituting the electric field, Eq. (1), and the density profiles, Eq. (3), into Eqs. (2a)–(2b) results in

$$\frac{\partial n}{\partial t} = -\tau_d^{-1} n \frac{F-1}{F} + \nu_{\text{att}} n_e - \gamma_d n, \quad (4a)$$

$$\frac{\partial p}{\partial t} = -\tau_d^{-1} p \left(\frac{F+1}{F} \right), \quad (4b)$$

$$\text{where } F = 1 + \frac{\mu_i}{\mu_e} \frac{p+n}{n_e}. \quad (4c)$$

During the first stage of the afterglow, the electron density is relatively large (Figs. 1 and 2), F is close to unity, negative-ion diffusive losses are small, and the positive-ion ambipolar diffusion coefficient is two times D_p .

In the late afterglow, electron and ion densities are coupled to each other and evolve in a similar manner $\partial p/p \partial t = \partial n/n \partial t$ (see Figs. 1 and 2 for times longer than 0.25 ms). Equations (4a)–(4c) can be combined to obtain a quadratic equation for inverse electronegativity, $y \equiv n_e/n$.

$$\tilde{\nu}_{\text{att}} y^2 + (1 - \tilde{\gamma}_d) y - 2\tilde{\gamma}_d \frac{\mu_i}{\mu_e} = 0, \quad (5)$$

where $\tilde{\gamma}_d \equiv \gamma_d \tau_d / 2$, $\tilde{\nu}_{\text{att}} \equiv \nu_{\text{att}} \tau_d / 2$. Equation (5) has two roots, one of which is negative and thus nonphysical. If $\tilde{\gamma}_d < 1$, neglecting terms of order μ_i/μ_e , $y = [2\tilde{\gamma}_d / (1 - \tilde{\gamma}_d)] \mu_i/\mu_e$, the electronegativity $n/n_e \sim \mu_e/\mu_i$ is large,

and the charged species fluxes correspond to free-electron and ion diffusion. The corresponding ratios of wall fluxes are $\Gamma_e/\Gamma_p = 2\tilde{\gamma}_d/(1 + \tilde{\gamma}_d)$ and $\Gamma_n/\Gamma_p = (1 - \tilde{\gamma}_d)/(1 + \tilde{\gamma}_d)$. Physically, this means that electrons are quickly removed by free diffusion. The electron flux in the late afterglow is produced by detachment of negative ions during their free diffusion. This implies that the electron flux is proportional to $\gamma_d \tau_d$. If $\tilde{\gamma}_d \geq 1$, the physical picture changes drastically. The solution to Eq. (5) is now $y = (\tilde{\gamma}_d - 1)/\tilde{\nu}_{\text{att}}$, and $\Gamma_e/\Gamma_p = 1$, $\Gamma_n/\Gamma_p = (\mu_i/\mu_e)(y+2)/2y(y+1)$. This corresponds to a relatively large number of electrons in the afterglow. The presence of these electrons causes the negative ions to be trapped. In the limit $\mu_i/\mu_e \rightarrow 0$, Equation (5) describes a transcritical bifurcation.¹⁷

The simplified theory has several limitations. The electron temperature in the afterglow (see Figs. 1 and 2) can be larger than the ion temperature (the latter is close to room temperature), ion mobilities can be different, and ion-ion recombination can play a role. Despite these limitations, the theory seems to capture the system behavior semiquantitatively. For example, the theory predicts the transition to take place at a value of $\gamma_d \tau_d = 2$, but numerical simulation (without the assumptions incorporated in the theory) predicts the transition to happen at a pressure of 3.5 mTorr, which corresponds to $\gamma_d \tau_d = 1.5$. Also, if $\gamma_d \tau_d$ is small, the analytical estimate of the flux ratio $\Gamma_e/\Gamma_n \approx \gamma_d \tau_d$ matches the simulation results (At $p = 2$ mTorr, $\gamma_d \tau_d = 0.55$, and simulation predicts $\Gamma_e/\Gamma_n = 0.499$; at $p = 1.5$ mTorr, $\gamma_d \tau_d = 0.28$, and simulation predicts $\Gamma_e/\Gamma_n = 0.3$). The reason for this close agreement could be the fact that, in spite of higher T_e , the electron density is too small in the late afterglow for the fields to be important.

In summary, negative ions can be extracted in the afterglow of electronegative discharges only if $\gamma_d \tau_d < 2$. This implies that negative-ion sources should operate at low pressures and not too large gaps.

¹T. H. Ahn, K. Nakamura, and H. Sugai, *Plasma Sources Sci. Technol.* **5**, 139 (1996).

²M. B. Hopkins and K. N. Mellon, *Phys. Rev. Lett.* **67**, 449 (1991).

³D. Hayashi and K. Kadota, *J. Appl. Phys.* **83**, 697 (1998).

⁴W. Swider, *Ionospheric Modeling* (Birkhauser, Basel, 1988).

⁵T. Takeuchi, S. Iizuka, and N. Sato, *Phys. Rev. Lett.* **80**, 77 (1998).

⁶I. D. Kaganovich and L. D. Tsendin, *Plasma Phys. Rep.* **19**, 645 (1993).

⁷I. Kaganovich, B. N. Ramamurthi, and D. J. Economou, *Phys. Rev. Lett.* **84**, 1918 (2000).

⁸V. Midha and D. Economou, *Plasma Sources Sci. Technol.* (to be published).

⁹B. A. Smith and L. J. Overzet, *Plasma Sources Sci. Technol.* **8**, 82 (1999).

¹⁰M. V. Malyshev, V. M. Donnelly, and S. Samukawa, *J. Appl. Phys.* **86**, 4813 (1999).

¹¹S. Ashida and M. A. Lieberman, *Jpn. J. Appl. Phys., Part 1* **36**, 854 (1997).

¹²M. A. Lieberman and A. J. Lichtenberg, *Principles of Plasma Discharges and Materials Processing* (Wiley, New York, 1994).

¹³U. Buddemeier, Ph.D. thesis, Ruhr Universitaet (1997).

¹⁴S. A. Gutsev, A. A. Kudryavtsev, and V. A. Romanenko, *Tech. Phys.* **40**, 1131 (1995).

¹⁵A. V. Phelps, *J. Res. Natl. Inst. Stand. Technol.* **95**, 407 (1990).

¹⁶M. V. Koniukov, *Sov. Phys. JETP* **12**, 629 (1958).

¹⁷J. Guckenheimer and P. Holmes, *Applied Mathematical Sciences* (Springer, Berlin, 1986), Vol. 42.